9

Wavelet-based techniques in MRS

A. Suvichakorn[a] *, H. Ratiney[b], S. Cavassila[b,†] and J.-P Antoine[a,‡]
[a]*Institut de physique théorique (FYMA), Université catholique de Louvain, B-1348 Louvain-la-Neuve, Belgium*
[b]*CREATIS-LRMN, CNRS UMR 5220, Villeurbanne F-69621 Inserm, U630, Villeurbanne F-69621; INSA-Lyon, Villeurbanne F-69621 Université de Lyon, Lyon, F-69003; Université Lyon 1, Villeurbanne F-69622 France*

1. Introduction: magnetic resonance spectroscopic (MRS) signals

A magnetic resonance spectroscopic (MRS) signal is made of several frequencies typical of the active nuclei and their chemical environments. The amplitude of these contributions in the time domain depends on the amount of those nuclei, which is then related to the concentration of the substance (Hornak, 1997).
This property is exploited in many applications of MRS, in particular in the clinical one. The MRS spectra contain a wealth of biochemical information characterizing the molecular content of living tissues (Govindaraju et al., 2000). Therefore, MRS is a unique non-invasive tool for monitoring human brain tumours, etc. (Devos et al., 2004), if it is well quantified.
When an MRS proton signal is acquired at short echo-time (TE), the distortion of spectral multiplets due to J-evolution can be minimized and the signals are minimally affected by transverse relaxation. Such signals exhibit many more metabolite contributions, such as glutamate and myo-inositol, compared to long TE spectra. Therefore, an MRS signal acquired at short TE presents rich *in vivo* metabolic information through complicated, overlapping spectral signatures. However, it is usually contaminated by water residue and a baseline which mainly originates from large molecules, known as macromolecules. As the shape and intensity of the baseline are not known *a priori*, this contribution becomes one of the major obstructions to accurately quantify the overlapping signals from the metabolites, especially by peak integration, which is commonly used in frequency-based quantification techniques. Also, by seeing only the frequency aspect, one loses all information about time localization.
A number of quantification techniques have been proposed, which work either in the time domain (see Vanhamme et al. (2001) for a review) or in the frequency domain (see Mierisová & Ala-Korpela (2001) for a review). The time-domain based methods are divided into two main classes: on one side, non-interactive methods such as SVD-based methods (Pijnappel et al., 1992) and, on the other side, methods based on iterative model function fitting using strong prior knowledge such as QUEST (Ratiney et al., 2004; 2005), LCModel (Provencher, 1993), AQSES (Poullet et al., 2007), or AMARES (Vanhamme et al., 1997).

*A. Suvichakorn is a Marie-Curie Research Fellow in the FAST (Advanced Signal Processing for Ultrafast Magnetic Resonance) Marie-Curie Research Network (MRTN-CT-2006-035801, http://fast-mrs.eu)
†*E-mail address*: Sophie.Cavassila@univ-lyon1.fr
‡*E-mail address*: Jean-Pierre.Antoine@uclouvain.be

However, there also exist techniques that analyse a signal in the two domains simultaneously and are therefore more efficient than, say, the Fourier transform, which gives only spectral information. The result is a time-scale and or a time-frequency representation, such as provided by the wavelet transform (WT) and the Short-Time Fourier transform (STFT). In addition, both transforms are local, in the sense that a small perturbation of a signal which may occur during the data acquisition will result only in a small, local modification of the transform.
A number of wavelet-based techniques have been proposed for spectral line estimation in MRS, including the continuous wavelet transform (Delprat et al., 1992; Guillemain et al., 1992; Serrai et al., 1997) and the wavelet packet decomposition (Mainardi et al., 2002). Among the various possibilities, we will concentrate our discussion on the continuous wavelet transform (CWT) with the Morlet wavelet (MWT). All wavelet calculations have been performed by our own wavelet toolbox, called YAWTb (Jacques et al., 2007). Some of the experimental aspects have been reported in Suvichakorn et al. (2009). For the convenience of the reader we have collected in the Appendix the basic features and properties of the CWT.
In the following sections, we will study the performance of the Morlet WT to retrieve parameters of interest such as resonances frequencies, amplitude and damping factors, for nuisances or impairments generally encountered in *in vivo* MRS signals: noise, baseline, solvent, and non-Lorentzian lineshapes.

2. The Morlet wavelet transform

The wavelet transform (WT) of a signal $s(t)$ with respect to a basic wavelet $g(t)$ is

$$\begin{aligned} S(\tau,a) &= \frac{1}{\sqrt{a}} \int \overline{g\left(\frac{t-\tau}{a}\right)}\, s(t)\, dt \\ &= \frac{1}{2\pi}\sqrt{a} \int \overline{G(a\omega)}\, S(\omega)\, e^{i\omega\tau}\, d\omega, \end{aligned} \tag{1}$$

where $S(\omega)$ is the Fourier transform of the signal, $a > 0$ is a dilation parameter that characterizes the frequency of the signal (since $1/a$ is essentially a frequency), $\tau \in \mathbb{R}$ is a translation parameter that indicates the localization in time and $\overline{G(a\omega)}$ is the complex conjugate of the (scaled) Fourier transform of $g(t)$. We can think of the basic wavelet as a window which slides through the signal, giving the information at instantaneous time τ. The window is also dilated by a, so that a small a corresponds to a high frequency of the signal, and *vice versa*. As a result, the WT becomes a function of both time and frequency (scale). For more details, see the Appendix.
A technique based on the continuous wavelet transform (CWT) was proposed by Guillemain et al. (1992). By exploiting the ability of the CWT to see the information in the two domains simultaneously, it can extract the information from MRS signals directly without any decomposition or pre-processing, in order to quantify an MRS signal. The technique proceeds in two steps: (i) detection of the frequency of the peaks in MRS signals and (ii) characterization at each detected frequency. It can be described as follows.
At a particular value of a, the WT $S_a(\tau) \equiv S(\tau, a)$ can be represented in terms of its modulus $|S_a(\tau)|$ and phase $\Phi_a(\tau)$, namely,

$$S_a(\tau) = |S_a(\tau)| e^{i\Phi_a(\tau)}, \tag{2}$$

with an instantaneous frequency

$$\begin{aligned}\Omega_a(\tau) &= \frac{\partial}{\partial\tau}\Phi_a(\tau)\\ &= \frac{\partial}{\partial\tau}\mathrm{Im}[\ln S_a(\tau)]\\ &= \mathrm{Im}\left[\frac{1}{S_a(\tau)}\frac{d}{d\tau}S_a(\tau)\right],\end{aligned} \tag{3}$$

Next, let us consider an MRS signal with a Lorentzian damping function, namely,

$$s_L(t) = Ae^{-Dt}e^{i(\omega_s t+\varphi)} \;\Leftrightarrow\; S_L(\omega) = 2\pi Ae^{i\varphi}\delta(\omega-(\omega_s+iD)), \tag{4}$$

where D and φ denote the damping factor and the phase of the signal. Its WT is accordingly

$$\begin{aligned}S_L(\tau,a) &= \sqrt{a}Ae^{i\varphi}e^{-D\tau}e^{i\omega_s\tau}\overline{G(a(\omega_s+iD))}\\ &= \sqrt{a}s(\tau)\overline{G(a(\omega_s+iD))}.\end{aligned} \tag{5}$$

For a Morlet function scaled by a dilation parameter a (we omit the negligible correction term, see Eq.(A.9)), namely,

$$G_M(a\omega) = \exp\left(-\tfrac{1}{2}\sigma^2(a\omega-\omega_0)^2\right), \tag{6}$$

it can be seen that the modulus of $S(\tau,a)$ is maximum, i.e., $\frac{\partial}{\partial a}S(\tau,a)\to 0$, when $\frac{\partial}{\partial a}G\to 0$. Given that $a>0$ and the assumption that $\omega_s \gg D$, the maximum can be found along the scale $a_r=\omega_0/\omega_s$ (this is called a *horizontal ridge*), which then gives

$$\overline{G_M(a_r(\omega_s+iD))} = \exp\left(\frac{\sigma a_r D}{\sqrt{2}}\right)^2, \tag{7}$$

and consequently

$$S_{a_r}(\tau) = \sqrt{a_r}\exp\left(\frac{\sigma a_r D}{\sqrt{2}}\right)^2 s(\tau), \tag{8}$$

which is identical to the signal $s(t)$ multiplied by a coefficient depending on the still unknown D. Consider the modulus of the Morlet wavelet transform (MWT) along a_r,

$$\begin{aligned}|S_{a_r}(\tau)| &= \sqrt{a_r}\exp\left(\frac{\sigma a_r D}{\sqrt{2}}\right)^2|s(\tau)|\\ \ln|S_{a_r}(\tau)| &= \frac{1}{2}\ln a+\left(\frac{\sigma a_r D}{\sqrt{2}}\right)^2+\ln A-D\tau.\end{aligned} \tag{9}$$

That is,

$$D = -\frac{\partial}{\partial\tau}\ln|S_{a_r}(\tau)|. \tag{10}$$

Knowing D can now lead to the estimation of the amplitude resonance A of the signal by

$$A = |s(t)|e^{Dt}. \tag{11}$$

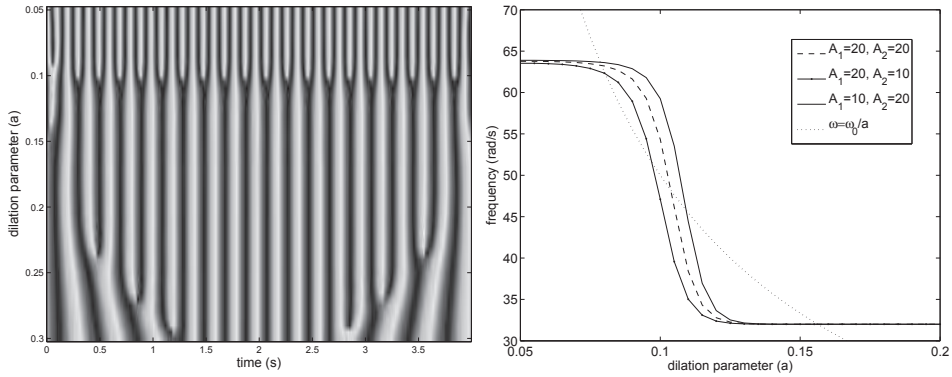

(a) (b)

Fig. 1. (a) Phase of the Morlet wavelet transform of a signal $s(t)$ containing two frequencies ω_s=32 and 64 rad/s and (b) its instantaneous frequency. Here $\sigma = 1, \omega_0 = 5$ rad/s, sampling frequency $F_s = 256\ \mathrm{s}^{-1}$, data length $l = 1024$ points.

Since $S_{a_r}(\tau)$ is a function of time, the derived D is also a function of time. This is beneficial for analysing signals that do not have a steady damping function. In addition, considering the phase of the MWT along a_r, namely,

$$\arg S_{a_r}(\tau) = \omega_s \tau + \varphi,$$

we also have

$$\begin{aligned} \omega_s &= \frac{\partial}{\partial \tau} \arg S_{a_r}(\tau) \\ &= \Omega_{a_r}(\tau), \end{aligned} \tag{12}$$

as in Eq.(3). Strictly speaking, the instantaneous frequency at the scale a_r of the Morlet transform is ω_s. This can be observed in Figure 1, which shows that the instantaneous frequency intersects the line ω_0/a at $a = \omega_0/\omega_s$, where ω_s=32 and 64 rad/s are the frequencies of the signal. The phase of the signal $\varphi \in (-\pi, \pi)$ can also be derived from the phase of the WT, if needed. The property given in Eq.(12) is useful for analysing an n-frequency signal; it indicates the actual frequencies of the signal and the scale a that we should consider. In addition, if its frequencies are *sufficiently* far away from each other, so that $\overline{G(a\omega)}$ treats each spectral line independently (Barache et al., 1997), the amplitude at each frequency can thus be derived. When two frequencies are very close to each other (this also depends on the sampling frequency), increasing the frequency of the Morlet function ω_0 can better localize and distinguish the overlapping frequencies. On the other hand, ω_s can be obtained iteratively by

1. Initializing $a = a_i$ at some values.
2. Calculating the instantaneous frequency, namely Ω_{a_i}.
3. Assigning the new value to $a_{i+1} = \omega_0/\Omega_{a_i}$.
4. Repeating the process until a converges to ω_s.

Figure 2 illustrates an overlap of two frequencies and the derived instantaneous frequencies using the iteration method. The derived frequencies converge to the true frequencies within a few steps.

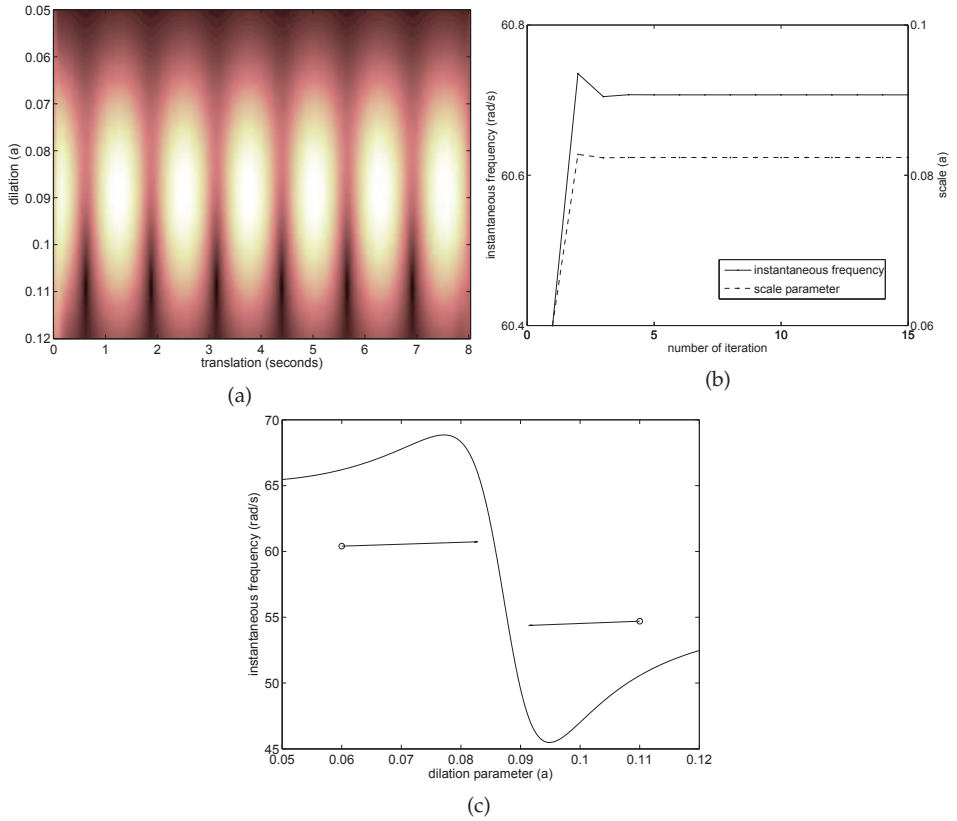

Fig. 2. (a) The MWT of $y(t) = \exp(i55t) + \exp(i60t)$ and (b) its instantaneous frequencies when using the iterative method. Here $\sigma = 1, \omega_0 = 5.5$ rad/s, $F_s = 800$ s^{-1}, $l = 1024$ points. (c) Comparison of the instantaneous frequencies by the non-iterative and the iterative method. The symbol $\circ$ indicates an initial value of a.

3. Continuous Wavelet Transform and the *in vivo* MRS challenges

3.1 Gaussian White Noise

An *in vivo* MRS signal is always impaired by additive noise, which is usually assumed to be white gaussian. This noise causes oscillations in the instantaneous frequency derived with the CWT representation, as illustrated in Figure 3 which shows the instantaneous frequency derived from a signal with a peak at a frequency of 32 rad/s with an additive Gaussian noise corresponding to a signal to noise ratio (SNR) of 10.[1] In order to reduce this effect, Guillemain

[1] The Signal to Noise ratio SNR is defined as the ratio of the time domain first point amplitude of the resonance to the time domain noise standard deviation

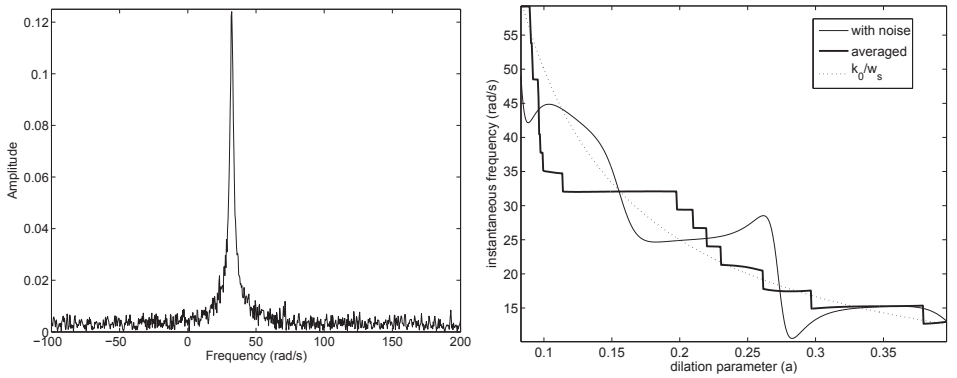

(a) (b)

Fig. 3. (a) A spectrum with one resonance at 32 rad/s with SNR=10 ($\sigma_n = 0.079$) and (b) its instantaneous frequency derived by the Morlet wavelet at $t = 4.7$ s ($\omega_0 = 5$ rad/s, σ=1, $Fs = 800\ \mathrm{s}^{-1}$).

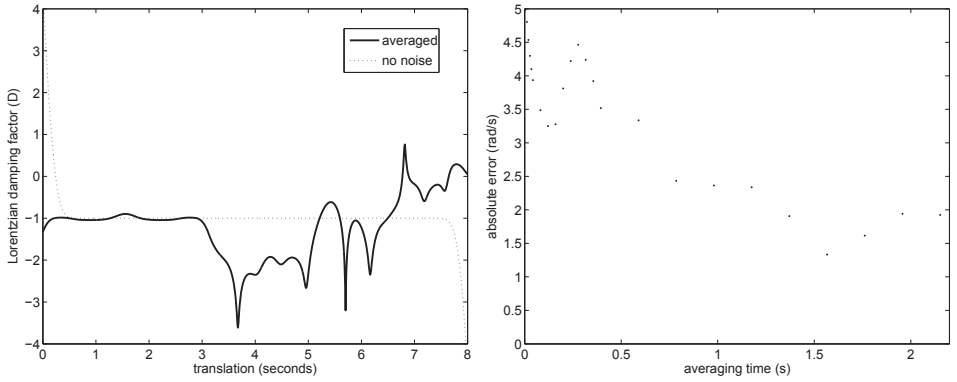

(a) (b)

Fig. 4. For the signal shown in Figure 3(a): Derived Lorentzian damping factor and (b) absolute frequency estimation error with respect to the averaging time, calculated at the scale $a = \omega_0/\omega_s$ of the Morlet wavelet transform (SNR = 10, ω_s = 32 rad/s,ω_0 = 5 rad/s, σ = 1, F_s = 800 s^{-1}).

et al. (1992) suggested averaging in time the derived parameters, for instance $\Omega_a(\tau)$, i.e.,

$$\overline{\Omega}_a = \frac{1}{T}\int_{\tau_0}^{\tau_0+T} \Omega_a(\tau)d\tau. \tag{13}$$

As can be seen in Figure 3, averaging in time reduces the noise effect on the derivation of the instantaneous frequency.[2] One can see that averaging creates many steady points. At the scale $a = \omega_0/32$, the instantaneous frequency is about, but not exactly, 32 rad/s. Here, the

[2] This property might be used for denoising, but this has not been exploited.

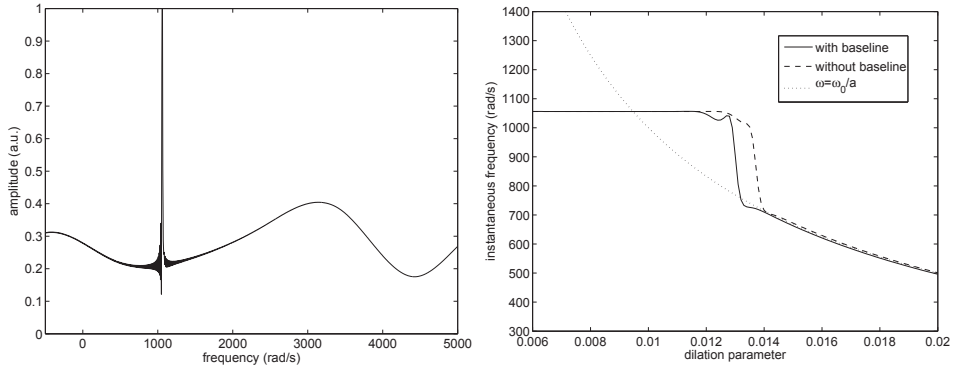

(a) (b)

Fig. 5. (a) The Fourier transform of a 1056-rad/s signal with baseline; b) Its instantaneous frequency ($\omega_0 = 10$ rad/s, $\sigma = 1$). The baseline is modelled by a cubic spline.

averaging time is 1.56 s. Figure 4(b) shows the evolution of the absolute frequency estimation with respect to the averaging time. Increasing the averaging time is likely to decrease the estimation error, as illustrated in Figure 4(b). The same approach can be used to derive the instantaneous damping factor. The estimated instantaneous damping factor is also smoother and closer to the actual damping factor when time averaging is employed. Although the method described above should work at any value of a, there is a particular range of a that is meaningful, and should be wisely selected. As a rule of thumb, this range should not be far from the scale that maximizes the modulus of the Morlet WT.

3.2 Baseline

The baseline corresponds to contributions from large molecules, with a broad frequency pattern in the MRS spectrum. Thus, it becomes a major obstruction in the quantification of metabolite contribution from the MRS signals. First, we simulate the baseline by cubic splines in order to study the performance of the MWT when a baseline is present. In the case of Figure 5, the simulated baseline has no effect on the instantaneous frequency derived from the WT. Then, we used a baseline modelled with 50 randomly distributed Lorentzian profiles with a large damping factor, compared to the signal-of-interest at 3447 rad/s, e.g. $s_L(t) = \exp(-10t)\exp(i3447t) + B(t)$ where $B(t) = \exp(-50t)[0.2\exp(i3447t) + 0.3\exp(i2000t) + \ldots]$ is the baseline (see Figure 6). The first component of $B(t)$ has the same frequency as the signal, in order to imitate the overlap between the baseline and the signal. It is found that the modelled baseline does not prevent an accurate estimation of both the damping factor and the amplitude derived from the Morlet WT, provided one waits until both the effect of the baseline and the edge effect (discussed in Section 4.1 below) have died out. In the example shown here, the waiting time is approximately 0.2 s.

The MWT in Figure 6(b) tells us that the baseline affects only the beginning of the transform in the time (τ) axis, comparing to the long, clear peak of our 3447-rad/s signal. This means that the baseline can be assumed to decay faster than the pure signal, and the method described should still be effective without removing the baseline beforehand. Such an assumption has been widely used in spectroscopic signal processing, where several authors have proposed truncation of the initial data points in the time domain, which are believed to contain a major

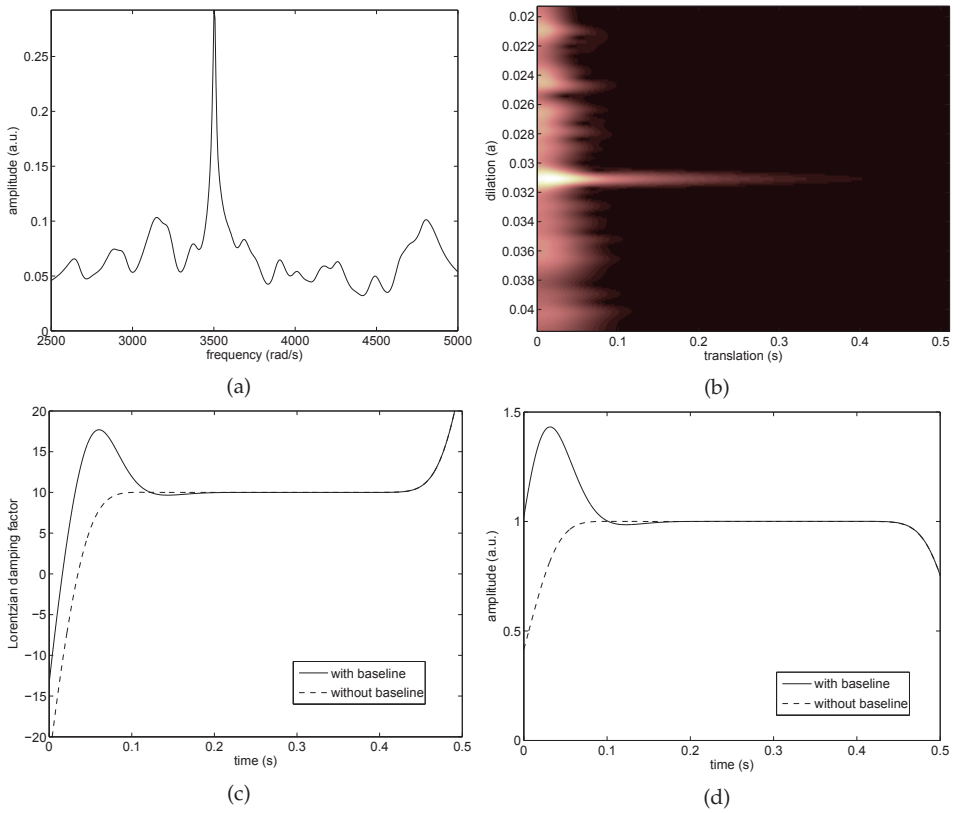

Fig. 6. (a) The Fourier transform of a 3447-rad/s Lorentzian signal with baseline. The latter is modelled by large Lorentzian damping factors; (b) Its Morlet WT and the derived parameters: (c) damping factor and (d) amplitude. The actual parameters are 10 s^{-1} and 1 a.u. for the damping factor and amplitude, respectively. ($\omega_0 = 100$ rad/s, $\sigma = 1$). From Suvichakorn et al. (2009).

part of the baseline. However, some information of the metabolites could be lost and a strategy for properly selecting the number of data points is needed (see Rabeson et al. (2006) for examples and further references).

Next, in order to study the characteristics of the real baseline by the Morlet wavelet, an *in vivo* macromolecule MRS signal was acquired on a horizontal 4.7T Biospec system (BRUKER BioSpin MRI, Germany). The data acquisition was done using the differences in spin-lattice relaxation times (T1) between low molecular weight metabolites and macromolecules (Behar et al., 1994; Cudalbu et al., 2009; 2007).

As seen in Figure 7, the metabolite-nullified signal from a volume-of-interest (VOI) central-

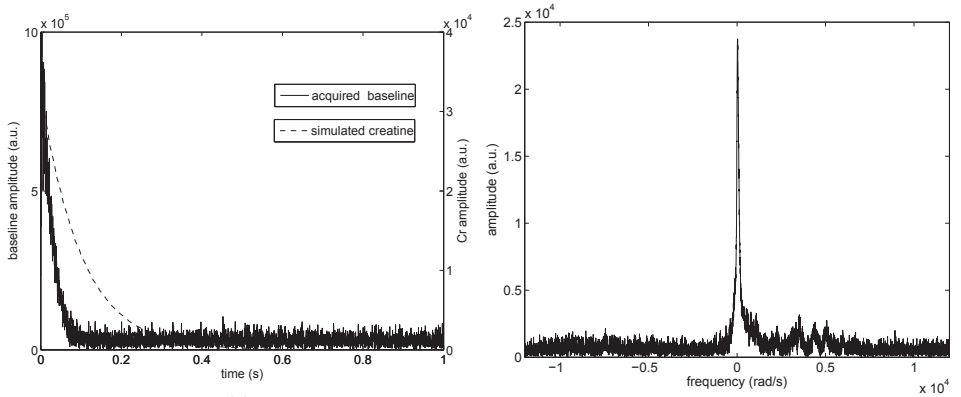

(a) (b)

Fig. 7. (a) The signal of baseline + residual water (a) in time domain; and (b) in frequency domain.

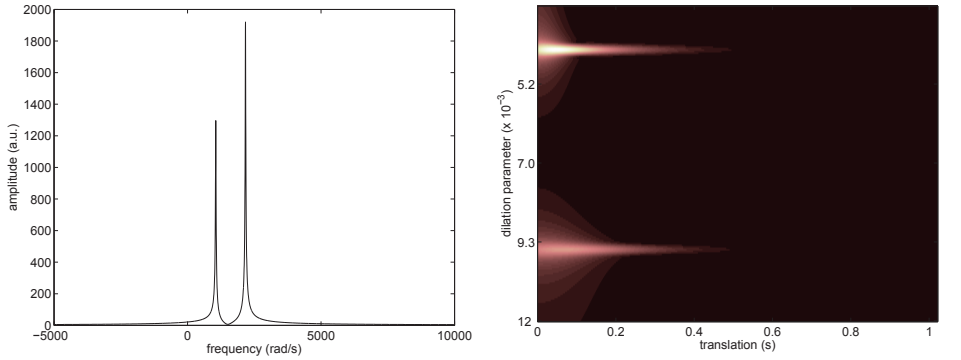

(a) (b)

Fig. 8. (a) Frequency response of creatine at 4.7 Tesla and (b) its Morlet WT (ω_0 = 10 rad/s, σ = 1, F_s = 4006.41 s^{-1}). The parameters derived from the Morlet transform are $D = 10\ s^{-1}$, $\omega_1 = 1056$ rad/s, $A_1 = 1330$ a.u. and $\omega_2 = 2168$ rad/s, $A_1 = 1965$ a.u.

ized in the hippocampus of a healthy mouse[3] resulted from a combination of residual water, baseline and noise. Compared to the simulated signal of creatine, whose frequency response and Morlet WT are shown in Figure 8, the signal decays much faster, making it suitable to use the Morlet wavelet to analyse the MRS signal as described earlier. For studying this, the two signals are normalised to the same amplitude and added together. Then the amplitude of the

[3] An Inversion-Recovery module was included prior to the PRESS sequence (echo-time = 20ms, repetition time = 3.5s, bandwidth of 4kHz, 4096 data-points) in order to measure the metabolite-nullified signal. The water signal was suppressed by variable power RF pulses with optimized relaxation delays (VAPOR). All first- and second-order shimming terms were adjusted using the Fast, Automatic Shimming technique by Mapping Along Projections (FASTMAP) for each VOI ($3 \times 3 \times 3$ mm^3). Inversion time = 700 ms.

creatine is derived with the Morlet WT. Next, we multiply the simulated, normalised creatine by 0.5, 1, 1.5,.... For each of these values, we derive the amplitude and plot the result in Figure 9. The recovery of the (simulated) creatine at different amplitudes, after adding it to the baseline signal, reveals that the amplitude of the metabolite can be correctly derived using $t = 0.4$ s, whereas at earlier time ($t < 0.2$ s) the derived amplitude still suffers from the boundary effect (we will discuss this effect in Section 4.1). However, the metabolite signal is covered later by noise ($t = 0.77$ s), giving an inaccurate amplitude estimate. Therefore, the time to monitor the amplitude of the metabolite should be properly selected. Another data set of the baseline[4] acquired at 9.4T, with a better signal to noise ratio and a better water suppression, shows similar characteristics (see Figure 10).

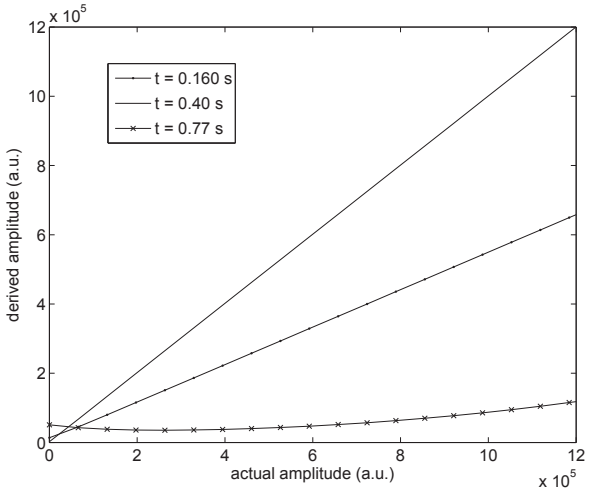

Fig. 9. Derived amplitude at $\omega = 1056$ rad/s, using $\omega_0 = 100$ rad/s and $\sigma = 1$ from a signal containing a simulated creatine signal and an *in vivo* acquired macromolecule signal.

3.3 Solvent

In MRS quantification, a large resonance from the solvent needs to be suppressed to unveil the metabolites without altering their magnitudes. The intensity of the solvent is usually several orders of magnitude larger than those of the metabolites.

[4] received from Cristina Cubaldu, Laboratory for Functional and Metabolic Imaging (LIFMET), Ecole Polytechnique Fédérale de Lausanne (EPFL).

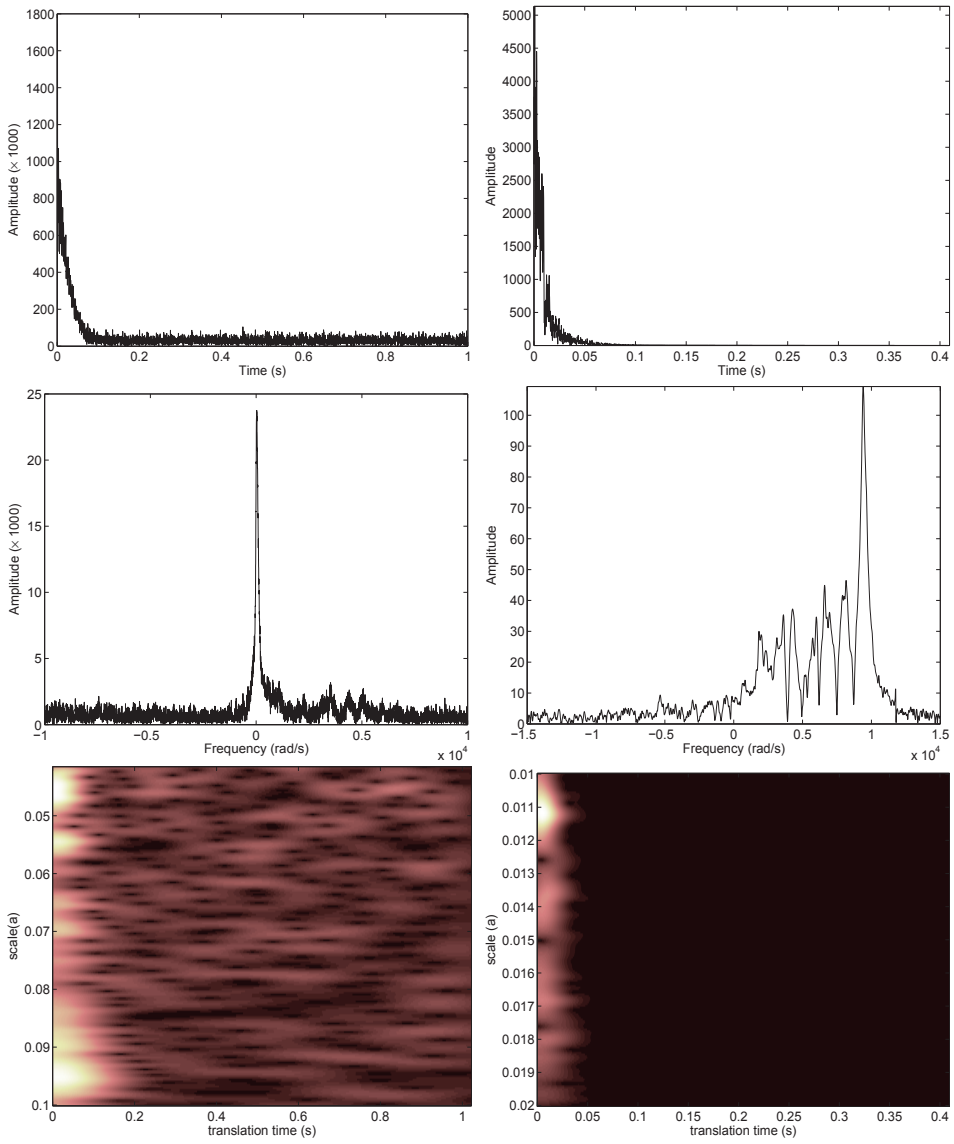

4.7 Teslas 9.4 Teslas

Fig. 10. Macromolecules MRS signals acquired at 4.7 Teslas and 9.4 Teslas, respectively, their Fourier transforms and their Morlet WT.

The Morlet WT sees the signal at each frequency individually, therefore it can work well even if the amplitudes at various frequencies are hugely different, which normally occurs when there is a solvent peak in the signal. In order to illustrate this, the Morlet WT has been applied

to the following signal

$$s(t) = 100e^{-8.5t}e^{i32t} + e^{-1.5t}e^{i60t} + e^{-0.5t}e^{i90t} + e^{-t}e^{i120t} + e^{-2t}e^{i150t}, \tag{14}$$

as seen in Figure 11 (a). This signal has an amplitude of 100 at 32 rad/s and 1 elsewhere. The high amplitude can affect other frequencies if they are close to each other. This is illustrated in Figure 11 (b) when a Hann window is applied to the signal in order to separate each frequency. Using the aforementioned method, the amplitude of 1 is derived as 0.980, 0.911, 0.988 and 0.974 respectively. The error ranges within 1.2-8.9 %, without any preprocessing.

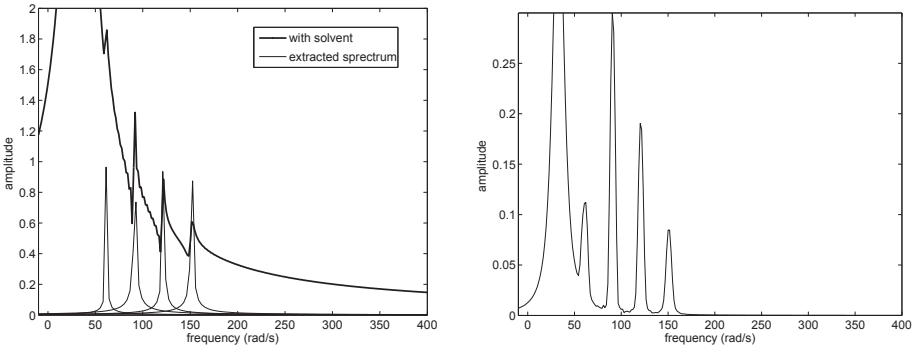

(a) (b)

Fig. 11. (a) The Fourier transform of a signal with different amplitudes and the spectrum extracted by the Morlet wavelet and (b) by a Hann window.

3.4 Non-Lorentzian lineshape

The ideal Lorentzian lineshape assumes that the homogeneous broadening is equally contributed from each individual molecule. However, imperfect shimming and susceptibility effects from internal heterogeneity within tissues lead to non-Lorentzian lineshapes in real experiments (Cudalbu et al., 2008). These effects are typically modelled by a Gaussian lineshape (Franzen, 2002; Hornak, 1997). Since the inhomogeneous broadening is often significantly larger than the lifetime broadening, the Gaussian lineshape is often dominant. If the lineshape is intermediate between a Gaussian and a Lorentzian form, the spectrum can be fitted to a convolution of the two functions (Marshall et al., 2000; Ratiney et al., 2008). Such lineshape is known as a *Voigt profile*.

Next we will explore how the Morlet WT can deal with the Gaussian and Voigt lineshapes. Consider a pure Gaussian function modulated at the frequency ω_s, namely,

$$s_G(t) = Ae^{-\gamma t^2}e^{i\omega_s t}. \tag{15}$$

Its Morlet WT is

$$\begin{aligned} S_G(\tau, a) &= \frac{1}{\sqrt{a}} \int \overline{g_M\left(\frac{t-\tau}{a}\right)} s_G(t)\, dt \\ &= \frac{A}{2\pi\sqrt{a}\sigma} \int e^{-\gamma t^2} e^{i\omega_s t} e^{-\left(\frac{t-\tau}{\sqrt{2}\sigma a}\right)^2} e^{-i\omega_0\left(\frac{t-\tau}{a}\right)} dt \\ &= \frac{A}{2\pi\sqrt{a}\sigma} \int e^{-(k_1 t^2 + k_2 t + k_3)} dt, \end{aligned} \tag{16}$$

where

$$k_1 = \gamma + \frac{1}{2\sigma^2 a^2}$$
$$k_2 = -i(\omega_s - \frac{\omega_0}{a}) - \frac{\tau}{\sigma^2 a^2}$$
$$k_3 = -i\frac{\omega_0 \tau}{a} + \frac{\tau^2}{2\sigma^2 a^2}.$$

Eq.(16) is known as a Gaussian integral and can be computed explicitly:

$$\int_{-\infty}^{\infty} e^{-(k_1 t^2 + k_2 t + k_3)} dt = \sqrt{\frac{\pi}{k_1}} e^{\frac{k_2^2}{4k_1} - k_3}. \tag{17}$$

As a result, the Morlet WT at the scale $a_r = \omega_0/\omega_s$ is

$$S_{G,a_r}(\tau) = k_4 A e^{-k_5 \tau^2} e^{i\omega_s \tau}, \tag{18}$$

where

$$k_4 = \sqrt{\frac{a_r}{2\pi(2\gamma\sigma^2 a_r^2 + 1)}}$$
$$k_5 = \frac{\gamma}{2\gamma\sigma^2 a_r^2 + 1},$$

which is also a Gaussian function at the frequency ω_s. The width and amplitude of this new Gaussian function are functions of ω_s and of the width of the original Gaussian signal $s_G(t)$. Therefore, similarly to the process of the Lorentzian lineshape, the amplitude (A) and the width of the Gaussian function (inversely proportional to γ) can be obtained as follows:

1. Find $\omega_s = \frac{\partial}{\partial \tau} \arg S_{G,a_r}(\tau)$.
2. Find γ from the second derivative of $\ln |S_{G,a_r}(\tau)|$, which yields

$$\gamma = -\frac{0.5}{\left(\frac{\partial^2}{\partial \tau^2} \ln |S_{G,a_r}(\tau)|\right)^{-1} + \sigma^2 a_r^2}. \tag{19}$$

3. Find A from the calculated ω_s and γ.

On the other hand, the Morlet WT at the scale $a_r = \omega_0/\omega_s$ of a Voigt lineshape,

$$s_V(t) = A e^{-\gamma t^2} e^{-Dt} e^{i\omega_s t}, \tag{20}$$

is given by

$$S_{V,a_r}(\tau) = k_6 A e^{-k_5(\tau - k_7)^2} e^{i\omega_s \tau}, \tag{21}$$

where

$$k_6 = k_4 e^{\frac{-D^2}{4\gamma}}$$
$$k_7 = \frac{D}{2\gamma}.$$

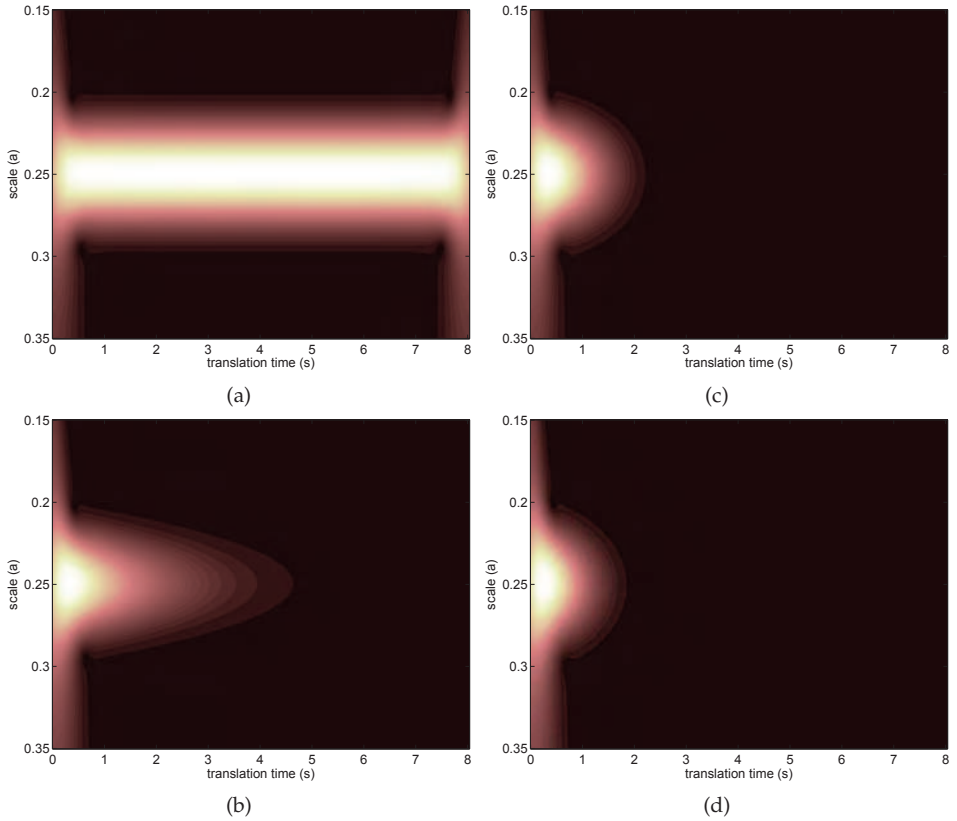

Fig. 12. (a) The modulus of the Morlet WT ($\omega_0 = 15$ rad/s) of a signal of a frequency 60 rad/s with (a) undamped $s(t) = e^{i60t}$; (b) Lorentzian $s(t) = e^{-t}e^{i60t}$; (c) Gaussian $s(t) = e^{-t^2}e^{i60t}$; and (d) Voigt $s(t) = e^{-t}e^{-t^2}e^{i60t}$ lineshape.

That is, at the scale a_r, the Morlet WT of the Voigt lineshape is also a Gaussian function with the same width, but shifted in time, with the amplitude smaller than that of the Gaussian lineshape, and its instantaneous frequency is also equal to ω_s.
Note that the scale $a_r = \omega_0/\omega_s$ does not give exactly the maximum modulus of the WT. However, as seen in Figure 12, the modulus of the Morlet WT of a signal with a Lorentzian lineshape or a Gaussian lineshape (and also a Voigt lineshape) are maximal at the same scale a_r, provided that $a \in \mathbb{R}$ and $\omega_s \gg D$.
Figure 13 shows that the second derivative of the modulus of the Morlet WT can be used to describe the second-order broadening of the lineshape, no matter whether it is Gaussian or Voigt. In the case of a Voigt lineshape, γ actually gives back a Lorentzian whose damping factor is obtained by Eq.(10).

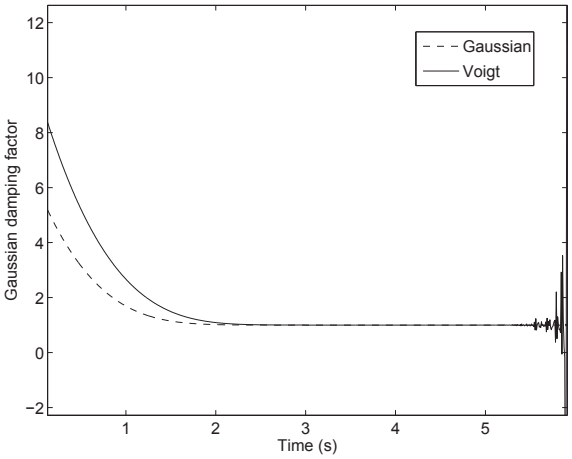

Fig. 13. The Gaussian damping factor derived from the pure Gaussian signal and the Voigt signal considered in Figure 12

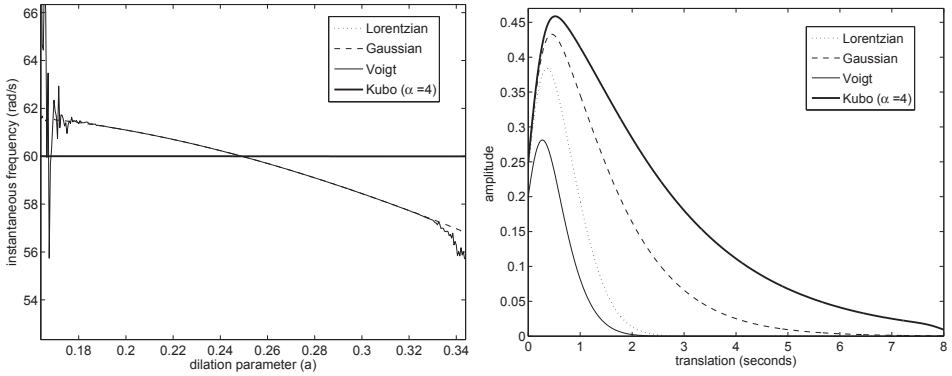

(a) (b)

Fig. 14. (a) The comparison of the derived instantaneous frequency of the Morlet WT of a signal of a frequency 60 rad/s with different lineshapes, e.g. Lorentzian $s(t) = e^{-t}e^{i60t}$, Gaussian $s(t) = e^{-t^2}e^{i60t}$, Voigt $s(t) = e^{-t}e^{-t^2}e^{i60t}$ and Kubo $s(t) = e^{-0.25(e^{-t}-1+t)}e^{i60t}$ at t= 4.7 s. Panel (b) shows the modulus of the Morlet WT of each line at $a_r = \omega_0/60$. Note: σ =1, ω_0 =15 rad/s, F_s = 800 s^{-1}, l = 1024 points.

Kubo's lineshape

The interaction between the Lorentzian and Gaussian broadening of lineshape depends on the time scale. For example, if the relaxation time (T_2) is much longer than any effect modulating the energy of a molecule, the lineshape will approach the Lorentzian lineshape. On the contrary, if T_2 is short, the lineshape is likely to be Gaussian. In order to account for this time

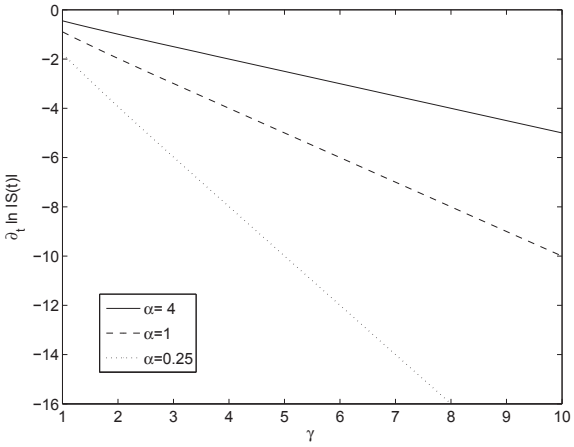

Fig. 15. $\frac{\partial}{\partial\tau}\ln|S_{G,a_r}(\tau)|$ with respect to Kubo's γ for the pure gaussian signal given in Eq.(15), at the scale $a_r = \omega_0/\omega_s$. We have put $\alpha = \gamma/\varsigma$, where γ and ς are the two parameters of the Kubo lineshape defined in Eq.(22).

scale, Kubo (1969) uses a so-called Gaussian-Markovian modulation, namely

$$s(t) = A\exp\big(-\frac{\varsigma^2}{\gamma^2}\left(e^{-\gamma t}-1+\gamma t\right)\big). \tag{22}$$

The parameter γ is inversely proportional to T_2 and ς is the amplitude of the solvent-induced fluctuations in the frequency. If $\alpha = \gamma/\varsigma \ll 1$, the lineshape becomes Gaussian, whereas $\alpha \gg 1$ leads to Lorentzian. The width of the lineshape is $\varsigma^2\gamma$.
Solving Eq.(22) seems to be complicated, though may be possible. However, it turns out that the maximum modulus of the Morlet WT of a Kubo lineshape at ω_s = 60 rad/s occurs also at the scale $a_r = \omega_0/\omega_s$, like those of the Gaussian and Lorentzian lineshapes. In addition, the instantaneous frequency is still able to derive the ω_s, even better than the Gaussian lineshape, as shown in Figure 14(a), although the amplitude is broader than those of the Lorentzian, Gaussian or Voigt profiles, as shown in Figure 14(b). The damping parameters can also be derived by the linear relation between $\frac{\partial}{\partial\tau}\ln|S_{G,a_r}(\tau)|$ and γ, as seen in Figure 15, whereas α is related directly to $\frac{\partial^2}{\partial\tau^2}\ln|S_{G,a_r}(\tau)|$.

4. Limitations of the Morlet wavelet transform

In the previous section, the Morlet WT shows its potential for analysing an MRS signal by means of its amplitude and phase, in addition to its time-frequency representation. However, these techniques can be applied to well-defined lineshapes only. Another limitation is the requirement of a proper ω_0 that should distinguish the signal from the solvent, but should not introduce noise in the result. In this section, we will look further on some more limitations that prevent the use of the Morlet WT to quantify MRS signals directly.

4.1 Edge effects

Errors in the wavelet analysis can occur at both ends of the spectrum due to the limited time series. The region of the wavelet spectrum in which effects become important[5] increases linearly with the scale a, thus it has a conic shape at both ends, as already seen in Figure 1(a) (see also the Appendix). The size of the forbidden region, which is affected by the boundary effect, varies with the frequency ω_0 of the Morlet wavelet function and the ratio between the frequency of the signal (ω_s) and the sampling frequency (F_s). Figure 16 shows that the size becomes larger for a large ω_0 and low ω_s/F_s. In practice, the working region is chosen so that the edge effects are negligible outside and the characterization of the MRS signals should be made inside this region, disregarding the presence of the macromolecular contamination.

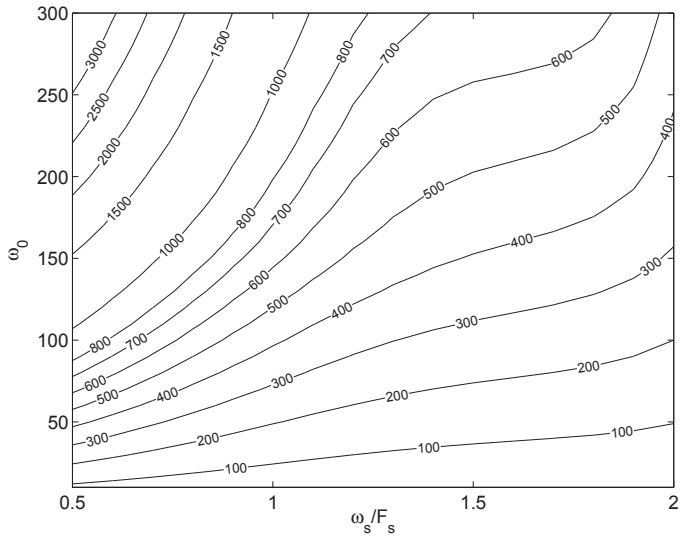

Fig. 16. Lines showing the width (in number of sample points) of the forbidden regions where the boundary effect becomes important, as a function of ω_0 (rad/s) and the ratio between the signal frequency (ω_s) and the sampling frequency (F_s). From (Suvichakorn et al., 2009).

4.2 Interacting/overlapping frequencies

If two frequencies of the signal are close to each other, the wavelet can interact with both of them at the same time. This was already observed in Figure 2(a). Barache et al. (1997) suggested the use of a linear equation system to solve the problem. In the sequel, the simulated N-Acetyl Aspartate (NAA) is used to illustrate how the problem could be solved. The spectrum of the NAA, shown in Figure 17(a), is composed of two different regions, the high, single peak (NAA–acetyl part) and a group of overlapping frequencies (NAA–aspartate part). By using a high ω_0 to separate the overlapping frequencies, the Morlet WT reveals that there are eight frequency peaks in the group as seen in Figure 17(b). The damping factors of the two parts of NAA are shown in Figure 18(a). Applying Eq.(10) directly to each peak causes an oscillation in the derived damping factor, compared to the smooth and stationary damping

[5] defined as the e-folding time for the autocorrelation of wavelet power at each scale.